General Relativity and Gravitation (2019) 51:156
https://doi.org/10.1007/s10714-019-2639-6

RESEARCH ARTICLE

The Kerr–Newman–(anti-)de Sitter spacetime: Extremal configurations and electrogeodesics

Jiří Veselý[1] · **Martin Žofka**[1]

Received: 17 June 2019 / Accepted: 11 November 2019

Abstract
We study motion of charged test particles, or electrogeodesics, in the Kerr–Newman–(anti-)de Sitter spacetime. We focus on the equatorial plane and the axis of symmetry where the analysis is considerably simpler. The electric charge opens up the possibility of new types of trajectories, particularly stationary points where the particle can remain indefinitely. It also influences the stability of the orbits, which can be interesting from the point of view of observations. We review the basic properties of the spacetime—the structure of its horizons, the extremal cases, the possibility of over-extreme rotation, regions admitting closed timelike curves, and the turnaround radius, among other.

Keywords Kerr–Newman–(anti-)de Sitter · Extreme horizons · Electrogeodesics · Effective potential

1 Introduction

Since the beginnings of general relativity, study of the geodetic structure has been used extensively to reveal the physical interpretation of spacetimes. Indeed, already the Schwarzschild solution requires us to follow the motion of test particles to ascertain that the apparent singularity of the surface located at $r = 2M$ is due to our poor choice of coordinates and can be covered by a smooth coordinate patch. The Schwarzschild solution describing a single, static black hole that inhabits the vacuum of an otherwise empty universe is obviously not very suitable when trying to describe real astrophysical objects. It is of interest that if we include electric charge, providing thus hair for the black hole, its causal structure and the character of its singularity change dramatically.

✉ Martin Žofka
zofka@mbox.troja.mff.cuni.cz

Jiří Veselý
jiri.vesely@utf.mff.cuni.cz

[1] Faculty of Mathematics and Physics, Institute of Theoretical Physics, Charles University, Prague, Czech Republic

Published online: 21 November 2019

The most significant step in this direction, however, was the addition of rotation by Kerr in 1963, yielding the stationary Kerr black hole of a geodesic structure similar to the charged solution. A succession of black-hole spacetimes have been introduced [1] and analyzed in detail from the point of view of motion of test particles—Schwarzschild, Reissner–Nordström, Kerr, Kerr–Newman [2–4], and their analogues including either a positive or a negative cosmological constant, which drastically changes the asymptotic properties of the solutions. Geodesics have also been discussed in some related spacetimes such as Kerr–Newman–Taub-NUT [5] and rotating, charged black-hole spacetime in $f(R)$ gravity [6].

In this paper we study the most general member of this black-hole family—the Kerr–Newman–(anti-)de Sitter spacetime. Unlike the other black-hole solutions in the family, the spacetime can feature a triple horizon depending on the particular set of its parameters. We include both null and timelike trajectories, which have already been discussed in [6], but we consider particles carrying a non-zero charge which interact with the spacetime not only gravitationally but also through the electromagnetic force. The charge enables the existence of new families of orbits, particularly static ones, which—in principle—can be observed, constraining thus the parameters of the central black hole.

The case of $\Lambda = 0$ shall not be discussed in this work as the properties of the Kerr–Newman solution are well known and its electrogeodesics have already been examined thoroughly [7]. We thus focus on the KN(a)dS solution, starting with a general discussion of its properties in Sect. 2. The spacetime has a richer structure of extreme configurations than simpler solutions and we discuss the possible cases in Sect. 3. We look at what happens with the horizons if we perturb the parameters of the black hole and we compare the configurations to the simpler Kerr black holes. We then examine the interesting trajectories corresponding to closed time-like curves in the brief Sect. 4. Finally, the most extensive Sect. 5 is devoted to an analysis of electrogeodesics. It discusses the integrals of motion, possible static positions of test particles, and general motion in the equatorial plane and along the axis, introducing an effective potential. We also touch on the problem of the turnaround radii.

2 The spacetime

The spacetime we shall be investigating is the Kerr–Newman–(anti-)de Sitter solution (KN(a)dS) with the standard Boyer–Lindquist-type coordinates [8,9]. The line element reads

$$\begin{aligned} \mathrm{d}s^2 = &-\frac{\Delta_r}{\Xi^2\rho^2}\left(\mathrm{d}t - a\sin^2\theta\,\mathrm{d}\phi\right)^2 + \frac{\rho^2}{\Delta_r}\mathrm{d}r^2 + \frac{\rho^2}{\Delta_\theta}\mathrm{d}\theta^2 \\ &+ \frac{\Delta_\theta \sin^2\theta}{\Xi^2\rho^2}\left(a\mathrm{d}t - (r^2+a^2)\mathrm{d}\phi\right)^2, \end{aligned} \tag{1}$$

where

$$\rho^2 = r^2 + a^2\cos^2\theta\,, \tag{2}$$

$$\Delta_r = (r^2 + a^2)\left(1 - \frac{1}{3}\Lambda r^2\right) - 2mr + q^2 \,, \tag{3}$$

$$\Delta_\theta = 1 + \frac{1}{3}\Lambda a^2 \cos^2\theta \,, \tag{4}$$

$$\Xi = 1 + \frac{1}{3}\Lambda a^2 \,. \tag{5}$$

This spacetime describes a rotating electrically-charged black hole with mass m, angular momentum per unit energy a and charge q in a background universe with a non-zero cosmological constant Λ. The orientation of the ϕ coordinate is chosen in such a way that angular momentum a is positive. The spacetime has a ring singularity located at $r = 0, \theta = \pi/2$. It is a stationary and axially-symmetrical electrovacuum solution of the Einstein–Maxwell equations with the four-potential [1]

$$\mathbf{A} = -\frac{qr}{\Xi\rho^2}\left(\mathrm{d}t - a\sin^2\theta\,\mathrm{d}\phi\right). \tag{6}$$

In order to retain the Lorentzian signature of the metric for all $\theta \in [0, \pi]$, we require

$$\frac{1}{3}\Lambda a^2 > -1 \Leftrightarrow \Xi > 0. \tag{7}$$

Then, $\Delta_\theta(\theta)$ is always positive. If $\Lambda > 0$, this condition is irrelevant as it is fulfilled for any a.

The solution can contain up to four distinct horizons, which can be found as the roots of $\Delta_r(r)$. Aside from the inner and outer black hole horizons R_I and R_O, which can be found in spacetimes of the Kerr and Reissner–Nordström families even for a vanishing Λ, for a positive Λ two so-called cosmological horizons $R_{\mathrm{C}-}$ and $R_{\mathrm{C}+}$ appear. If all four horizons are present, their radii fulfill

$$R_{\mathrm{C}-} < 0 < R_\mathrm{I} < R_\mathrm{O} < R_{\mathrm{C}+}. \tag{8}$$

However, for a particular combination of the spacetime's parameters, certain horizons may merge, leading to extremal scenarios, or disappear altogether.

Furthermore, due to the presence of the cosmological term, this solution is not asymptotically flat, unlike the simpler black hole models. Current observations [10] suggest that we live in a universe with a positive cosmological parameter

$$\Omega_\Lambda \equiv \frac{\Lambda c^2}{3H_0^2} = 0.6889 \pm 0.0056, \tag{9}$$

where $H_0 = (67.66 \pm 0.42)$ km s^{-1} Mpc^{-1} is the present-day Hubble parameter. From there, we get

$$\Lambda = (1.11 \pm 0.02)\, 10^{-52}\ \mathrm{m}^{-2}. \tag{10}$$

[1] There is a typo in [9]: the inclusion of a non-zero cosmological constant in the Kerr–Newman solution does require the four-potential to be divided by $\Xi(\Lambda)$.

However, the most massive astrophysical black holes ever observed have masses of the order of [11]

$$M_{\max}^{\mathrm{BH}} = 10^{10} M_{\odot} \approx 1.5 \times 10^{13}\,\mathrm{m}. \tag{11}$$

As astrophysical black holes satisfy $a \lesssim m$, then

$$\Lambda a^2 \lesssim \Lambda m^2 \lesssim \Lambda \left(M_{\max}^{\mathrm{BH}}\right)^2 \approx 2.5 \times 10^{-26} \ll 1 \tag{12}$$

and Λ can therefore be treated locally as a perturbation of the Kerr–Newman metric. For it to have a measurable effect, we need $\Lambda r^2 > 1$, which occurs for sufficiently large radii.

Unlike the standard Euclidean spherical coordinates, the Boyer–Lindquist radial coordinate r is extended into negative values. These are hidden behind the black hole horizons (if there are any) within the inner region of the black hole. It is natural for us to assume that we live in the outer region, as a static observer in the area with negative r would be, among other things, always subjected to a naked singularity. We shall, therefore, place greater emphasis on positive values of r.

3 Extremal horizons

Before we move on to study electrogeodesics, we list some interesting properties of the extremal horizons possibly present in the KN(a)dS spacetimes. The corresponding spacetimes have a simpler causal structure and the number of their independent physical parameters is reduced, making thus the description of an extremal black hole simpler than that of a non-extremal black hole or a naked singularity. Furthermore, the proper distance from a point outside of a horizon to the horizon is finite for a simple horizon while it diverges for double and triple horizons. Another thing to note is that while horizon temperature of a simple horizon is non-zero and finite, temperatures of double and triple horizons vanish [12]. Extremality of black holes is due to the merging of their originally separate horizons. Therefore, in order to construct extreme black holes out of the KN(a)dS spacetime, we first need to analyze the horizons, which are the roots of $\Delta_r(r)$—a polynomial of degree four. For $\Lambda > 0$, it has at least one positive and at least one negative root while for $\Lambda < 0$ there may be no real roots. The higher the multiplicity of the horizons, the less independent parameters; for example, with a given positive cosmological constant[2] and a single triple horizon, there is just one more physical parameter, which may be taken to be the mass of the black hole. However, even these parameters may need to satisfy certain inequalities to represent physically acceptable spacetimes.

We describe the causal structure of the spacetime as, e.g., $(-1 \oplus 2 + 1-)$, telling us there is a single horizon at a negative r ($r = 0$ is denoted '$\oplus$'), followed by a double and a single horizons at positive r's. If a region between two neighboring horizons is stationary we write '+' between the corresponding numbers, or we write '−' if it is non-stationary (the region around $r = 0$ is always stationary, whence '$\oplus$') and

[2] We generally prefer to keep Λ as a free parameter because, from the astrophysical point of view, its value is known and fixed for all black holes.

Table 1 The three extremal families in KN(a)dS with a horizon of multiplicity two

Scenario	$(-1 \oplus 2 + 1-)$	$(-1 \oplus 1 - 2-)$	$(\oplus 2+)$
Parameters	$\Lambda > 0$	$\Lambda > 0$	$\Lambda < 0$
	$a^2 \in \left[0, \frac{21-12\sqrt{3}}{\Lambda}\right]$	$a^2 \in \left[0, \frac{21-12\sqrt{3}}{\Lambda}\right]$	$a^2 \in \left[0, \frac{3}{\lvert\Lambda\rvert}\right)$
	$q^2 \in \left[0, \frac{9-42a^2\Lambda+a^4\Lambda^2}{36\Lambda}\right]$	$q^2 \in \left[0, \frac{9-42a^2\Lambda+a^4\Lambda^2}{36\Lambda}\right]$	$q^2 \in [0, \infty)$
	$m = \frac{\Lambda\alpha_+^2\beta_-}{3}$	$m = \frac{\Lambda\alpha_-^2\beta_+}{3}$	$m = \frac{\Lambda\alpha_+^2\beta_-}{3}$
Horizons	$R_{1-} = -\alpha_+ - \beta_-$	$R_{1-} = -\alpha_- - \beta_+$	$R_2 = \beta_-$
	$R_2 = \beta_-$	$R_{1+} = +\alpha_- - \beta_+$	
	$R_{1+} = +\alpha_+ - \beta_-$	$R_2 = \beta_+$	
	$\alpha_\pm = \sqrt{\frac{1}{3\Lambda}\left(6 - 2a^2\Lambda \pm \sqrt{9 - 42a^2\Lambda + a^4\Lambda^2 - 36\Lambda q^2}\right)}$		
	$\beta_\pm = \sqrt{\frac{1}{6\Lambda}\left(3 - a^2\Lambda \pm \sqrt{9 - 42a^2\Lambda + a^4\Lambda^2 - 36\Lambda q^2}\right)}$		

the same applies to the asymptotic regions. Apart from the doubly degenerate case discussed below, the solution admits three distinct families of extremal spacetimes containing one horizon of multiplicity two. The required parameter combinations are listed in Table 1, along with the positions of the horizons.

The most interesting case is $(-1 \oplus 3-)$, the causal structure of which is shown in Fig. 1. This is a spacetime containing a doubly degenerate horizon, which can only occur in the present family of spacetimes if none of its parameters m, a, q, Λ vanishes. If we choose Λ and m as our parameters, then for the single horizon located at $r = R_1$ and the triple horizon at $r = R_3$ we can write

$$R_1 = -3R_3, \quad R_3 = \sqrt[3]{\frac{3}{4}\frac{m}{\Lambda}}, \tag{13}$$

while

$$\Lambda > 0, \quad m^2 \in \left[\frac{16(26\sqrt{3} - 45)}{3\Lambda}, \frac{2}{9\Lambda}\right], \tag{14}$$

and

$$a^2 = \frac{3}{\Lambda} - 6R_3^2, \qquad q^2 = \Lambda R_3^4 - a^2. \tag{15}$$

With a vanishing cosmological constant, extremal spacetimes from the Kerr(–Newman) or Reissner–Nordström families form the boundary between the two-horizon scenarios and naked singularities with no horizons. Extremal scenarios play a similar role for a non-vanishing Λ as well, which can be shown by computing the derivatives of Δ_r with respect to the spacetime parameters. We find that as we change the parameters of the metric a double root of Δ_r either splits into two separate ones or disappears altogether while a triple root always becomes a single root. The results of parametric perturbations can be found in Table 2, using the established notation of horizon configurations.

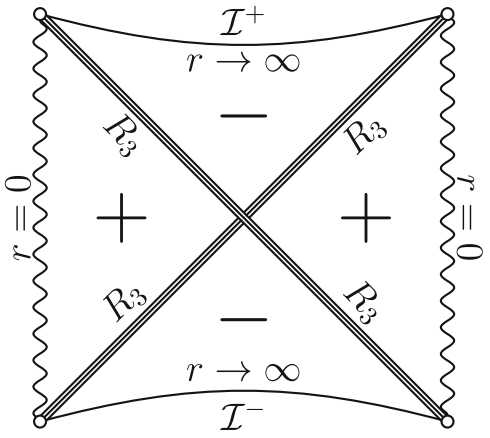

(a) $\theta = \pi/2$

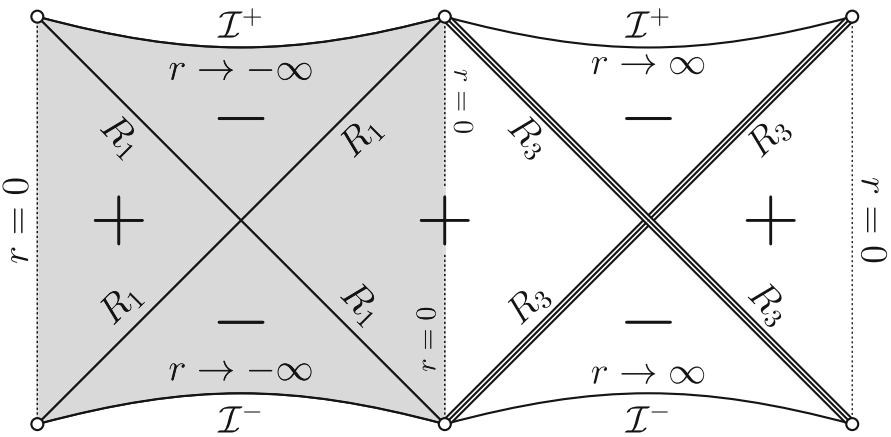

(b) $\theta \neq \pi/2$

Fig. 1 Conformal diagrams of a scenario $(-1 \oplus 3-)$ black hole for a given θ. The '+' and '−' signs denote the sign of Δ_r, i.e., whether the given area is stationary or dynamical, respectively. The area with $r < 0$ is grayed out. Maximal analytical extension is achieved by joining multiple copies of diagram **b** along the lines with $r = 0$

Table 2 Perturbations of extremal horizons due to a change in Δ_r at the location of the extremal horizon. There, Δ_r increases with increasing a and $|q|$ and with decreasing Λ and m

Extremal	Increased Δ_r	Decreased Δ_r
$(-1 \oplus 3-)$	$(-1 \oplus 1-)$	$(-1 \oplus 1-)$
$(-1 \oplus 2+1-)$	$(-1 \oplus 1-)$	$(-1 \oplus 1-1+1-)$
$(-1 \oplus 1-2-)$	$(-1 \oplus 1-1+1-)$	$(-1 \oplus 1-)$
$(\quad \oplus 2+)$	$(\quad \oplus)$	$(\quad \oplus 1-1+)$

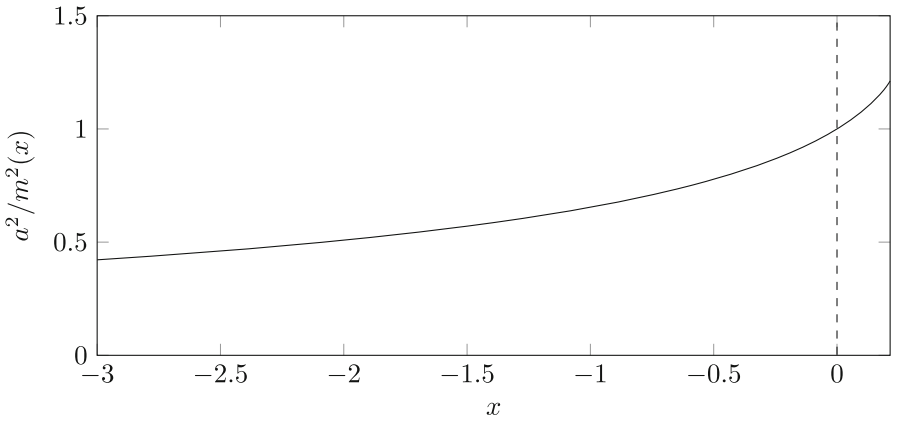

Fig. 2 The dependence of a^2/m^2 on $x \equiv \Lambda a^2$ for the permitted values of x for the Kerr-like extremal black holes of the Kerr–(anti-)de Sitter family

A commonly used model for astrophysical black holes is the Kerr spacetime [13]. For that spacetime to represent an actual black hole it must hold that $m \geq a$. Observations of astrophysical black holes seem to agree with this fact so far, even though there are black holes nearing extremality [14–16]. The Kerr metric, however, does not include the cosmological constant. It may, therefore, be of astrophysical relevance to see if real black holes can satisfy $m < a$ by adding Λ to the model.

The extremal KN(a)dS scenarios corresponding to the Kerr spacetime are $(\oplus 2+)$ and $(-1 \oplus 2 + 1-)$, as the other ones are naked. Astrophysically relevant is the latter scenario, as it includes a positive Λ in accordance with current observations, while the former includes a negative Λ. Conveniently, the expression for mass $m(\Lambda, a, q)$ is the same in both cases, see Table 1. We want to examine the highest possible specific angular momentum of the extremal black hole. To this end, we introduce a new parametrization $x \equiv \Lambda a^2$ and $y \equiv \Lambda q^2$, writing

$$\frac{a^2}{m^2} = \frac{486x}{\left(3-x-\sqrt{9-42x+x^2-36y}\right)\left(6-2x+\sqrt{9-42x+x^2-36y}\right)^2}, \quad (16)$$

where for $(-1 \oplus 2 + 1-)$ it holds that $x \in \left[0, 21 - 12\sqrt{3}\right]$ and $y \in \left[0, \frac{9-42x+x^2}{36}\right]$, while for $(\oplus 2+)$ we have $x \in (-3, 0]$ with $y \in (-\infty, 0\,]$. The ratio a^2/m^2 is a decreasing function of y within the entire domain for $(-1 \oplus 2 + 1-)$ while it is an increasing function for $(\oplus 2+)$ so in order to maximize it, we must put $y = 0$ in both cases, restricting thus the spacetime to the K(a)dS. The resulting ratio for the entire allowed interval $x \in (-3, 21 - 12\sqrt{3}]$ is plotted in Fig. 2.

Regarding the astrophysically relevant scenario $(-1 \oplus 2 + 1-)$, from the right part of the chart we can see that an extremal black hole necessarily is over-rotating for any permitted value of $x > 0$. Thus the highest angular momentum of a charged rotating

black hole with a cosmological constant is

$$\lim_{a\to a_{\max}} \frac{a^2}{m^2} = \frac{3}{16}(3+2\sqrt{3}) \approx 1.21, \tag{17}$$

with $a^2_{\max} = (21-12\sqrt{3})/\Lambda$, identical to the KdS spacetime, see [17]. Astrophysical black holes thus can satisfy $a > m$ without being naked singularities, but do they in reality?

Considering the cosmological constant of our universe (10), we can see that (omitting the considerably smaller error intervals)

$$a_{\max}\Big|_{\Lambda=1.11\times10^{-52}\,\mathrm{m}^{-2}} \approx 4.4\times10^{25}\,\mathrm{m} \tag{18}$$

with the corresponding mass

$$m \approx 4.0\times10^{25}\,\mathrm{m} \approx 2.7\times10^{22} M_\odot. \tag{19}$$

However, the most massive black holes ever observed have masses of the order of $M^{\mathrm{BH}}_{\max} = 10^{10} M_\odot$, (11), which is well below our result computed using $a_{\max}$ by 12 orders of magnitude. For these black holes, expressing a from the formula for m and using the measured value of Λ, $q = 0$ and $m = M^{\mathrm{BH}}_{\max}$, we obtain $a^{\mathrm{BH}}_{\max}$ practically equal to $M^{\mathrm{BH}}_{\max}$. As expected, $a^{\mathrm{BH}}_{\max}$ is smaller than $a_{\max}$ by 12 orders, and we can thus effectively consider the limit $x \to 0$ for any observed black hole. Astrophysical black holes, therefore, satisfy $m \geq a$, as is valid for black holes of the Kerr family. A theoretical deviation from this condition is negligible and would require very precise observations in order to be measured. However, even though none has been found yet, one should never exclude the possibility of the existence of black holes massive enough to be actually able to satisfy $m < a$...

In the $(\oplus 2+)$ case with $\Lambda < 0$, the extremal black holes actually satisfy $a^2/m^2 < 1$, see Fig. 2. Spin up the black hole as much as possible to obtain

$$\lim_{a^2\to -3/\Lambda} \frac{a^2}{m^2} = \frac{27}{64} \approx 0.42, \tag{20}$$

which, perhaps paradoxically, represents the lowest value possible for this type of extremal black holes.

4 Closed timelike curves

In the Kerr solution closed timelike curves (CTC's) can be found only in the part of the spacetime with a negative r coordinate. With the addition of the black hole's charge in the Kerr–Newman solution, however, they also appear in the area with positive r around the singularity, which is true for the KN(a)dS as well. It is of interest that for the general KN(a)dS it is possible to prove analytically that they must lie below

the innermost black hole horizon (even below the inner ergosphere), hidden thus from outside observers, which is rather reassuring since these paths allow observers following them to travel backwards in time, possibly violating causality. Fortunately, according to the chronological censorship hypothesis nature seems to have its way of disarming these curves (see, e.g., [18,19]), which is indeed the case here. A proof limited to the equatorial plane of the Kerr–Newman spacetime can be found in [20]. Our spacetime, however, is more general and we admit completely general motion of the test particles.

CTC's are located in the area where $g_{\phi\phi} < 0$. Looking at the expression for $g_{\phi\phi}$,

$$g_{\phi\phi}(r,\theta) = \frac{\sin^2\theta}{\Xi^2\rho^2(r,\theta)}\Big(\Xi r^4 + \Xi a^2(1+\cos^2\theta)r^2 + 2ma^2(1-\cos^2\theta)r + \Xi a^4\cos^2\theta + a^2q^2(\cos^2\theta - 1)\Big), \quad (21)$$

this happens if and only if

$$G(r,\theta) \equiv \frac{\Xi^2\rho^2(r,\theta)}{\sin^2\theta} g_{\phi\phi}(r,\theta) = \Xi r^4 + \Xi a^2(1+\cos^2\theta)r^2 + 2ma^2(1-\cos^2\theta)r + \Xi a^4\cos^2\theta + a^2q^2(\cos^2\theta - 1) \quad (22)$$

is also negative. Since $\Xi > 0$ (7) it is clear that

$$\frac{\partial G(r,\theta)}{\partial r} = 4\Xi r^3 + 2\Xi a^2(1+\cos^2\theta)r + 2ma^2(1-\cos^2\theta) \quad (23)$$

is positive everywhere for $r > 0$, which means that $G(r,\theta)$ increases monotonically with increasing $r > 0$. Because the function is continuous, there is at most one positive root for a given θ, provided that for this θ the function was negative at $r = 0$ in the first place,

$$G(r=0,\theta) = \Xi a^4\cos^2\theta + a^2q^2(\cos^2\theta - 1). \quad (24)$$

Take note that because of the presence of $1/\rho^2$, $g_{\phi\phi}$ actually diverges at the singularity, but the sign is nevertheless given by the sign of G.

Hence, to see that CTC's indeed lie below the inner ergosphere (defined by $g_{tt} > 0$) it suffices to show that at its boundary (i.e., $\bar{r}(\theta)$ for which $g_{tt}(\bar{r},\theta) = 0$), the function $G(\bar{r},\theta)$ is non-negative. One could do this by expressing m from

$$g_{tt}(\bar{r},\theta) = \frac{1}{3\Xi^2\rho^2(\bar{r},\theta)}\Big(\Lambda\bar{r}^4 + (\Lambda a^2 - 3)\bar{r}^2 + 6m\bar{r} - 3q^2 + \Lambda a^4(1-\cos^2\theta)\cos^2\theta - 3a^2\cos^2\theta\Big) = 0 \quad (25)$$

and inserting it into (22) to obtain

$$G(\bar{r},\theta) = \rho^2(\bar{r},\theta)\Delta_\theta(\theta)\Big(\bar{r}^2 + a^2(2-\cos^2\theta)\Big), \quad (26)$$

which is manifestly non-negative for $\forall\,\theta$ (recall that $\Delta_\theta > 0$).

Take note that for certain values of the parameters in the metric both the black-hole horizons and the ergosphere may vanish. In such a case an external observer could

see both the singularity and the CTC's. For a discussion of some special families of CTC trajectories in naked-singularity spacetimes, see [21] for Kerr and [22] for Kerr–Newman. If we take seriously the cosmic censorship hypothesis and discard the naked-singularity class of KN(a)dS spacetimes, then we automatically also have chronology protection here since the CTC's are always below the black-hole horizon.

5 Electrogeodesics

To explore the physics of the KN(a)dS solution from a different point of view, we now turn our attention to the study of motion of test particles in the field generated by the black hole. Since the spacetime carries an electric charge it is natural to allow both neutral and charged test particles alike. We focus on some cases of particular interest, such as static points or circular orbits, using a Lagrangian density of the form [23]

$$\mathcal{L} = \frac{1}{2} g_{\mu\nu} \dot{x}^\mu \dot{x}^\nu + \kappa \dot{x}^\mu A_\mu, \tag{27}$$

where κ is the particle's charge-to-mass ratio and dot denotes derivative with respect to the affine parameter.

With the coordinate time t and angle ϕ being cyclic we immediately have two conserved quantities

$$-E \equiv \frac{\partial \mathcal{L}}{\partial \dot{t}} = g_{tt}\dot{t} + g_{t\phi}\dot{\phi} + \kappa A_t, \tag{28}$$

$$L \equiv \frac{\partial \mathcal{L}}{\partial \dot{\phi}} = g_{t\phi}\dot{t} + g_{\phi\phi}\dot{\phi} + \kappa A_\phi. \tag{29}$$

In analogy with asymptotically flat spacetimes, we shall call E the particle's energy and L its angular momentum parallel to the axis of rotation of the black hole although the studied spacetime is not asymptotically flat and the interpretation of the constants is not clear. We can further use the Hamilton–Jacobi approach, yielding a separated equation and the analogue of the Carter constant

$$\begin{aligned} &-\delta a^2 \cos^2\theta + \Delta_\theta(\theta)\big(\Theta'(\theta)\big)^2 + \frac{\Xi^2}{\Delta_\theta(\theta)\sin^2\theta}\left(L - Ea\sin^2\theta\right)^2 = \\ &= \delta r^2 - \Delta_r(r)\big(R'(r)\big)^2 + \frac{\Xi^2}{\Delta_r(r)}\left(La - E(a^2+r^2) + \frac{r}{\Xi}q\kappa\right)^2 \equiv K, \end{aligned} \tag{30}$$

where $\Theta(\theta)$ and $R(r)$ are separated components of the action and δ is the used normalization of the four-velocity—massive particles have $\delta = -1$ and photons have $\delta = \kappa = 0$. This generalizes the result for the simpler black holes discussed in [7,24]. As we shall deal with particles moving along the axis where $K|_{\theta=0} = -\delta a^2$ and within the equatorial plane with $K|_{\theta=\pi/2} = \Xi^2 (aE - L)^2$, the Carter constant does not contain any information additional to the above two integrals of motion.

5.1 The static case

First, we shall investigate particles static in the used coordinate system, with $\dot{x}^i = 0$. This can only happen at certain locations that must clearly exhibit some symmetry and we thus consider the equatorial plane and the axis where the only nontrivial electrogeodesic equation is the one for $\ddot{r}$, imposing conditions on the position of static particles.

On the axis, we have a single remaining equation of motion

$$\begin{aligned}&\Big[\Lambda s r^7 - \kappa q \Lambda r^6 + 3\Lambda a^2 s r^5 - 3(ms - \kappa q) r^4 + 3\left((a^4\Lambda + q^2)s - 2\kappa q m\right) r^3 \\ &+\kappa q (a^4\Lambda + 3q^2) r^2 + a^2\left((a^4\Lambda + 3q^2)s + 6\kappa q m\right) r \\ &+3a^2\left(a^2 m s - \kappa q (a^2 + q^2)\right)\Big]\Big[(a^2 + r^2)^3 s\Big]^{-1} = 0\end{aligned} \tag{31}$$

with

$$s = \sqrt{\frac{\Delta_r(r)}{\rho^2(r, \theta = 0)}}. \tag{32}$$

All particles static on the spacetime's axis in the used coordinate system are zero angular momentum observers, which is a coordinate-independent covariant staticity condition. Finding the static positions for a given particle in a given spacetime is a matter of numerical computations. However, an analytical result can be obtained if we instead look for a properly-charged particle that would remain still at a given r in a given spacetime, yielding

$$\kappa = -\frac{\Lambda r^5 + 2a^2\Lambda r^3 - 3mr^2 + (a^4\Lambda + 3q^2) r + 3a^2 m}{3q(r + a)(r - a)s}. \tag{33}$$

For a non-vanishing a, this relation suggests there are two special locations on the axis: for $r = \pm a$, the terms with κ in (31) vanish, and the rest of the equation is remarkably reduced to

$$\Lambda = -\frac{3}{4}\frac{q^2}{a^4}. \tag{34}$$

If the spacetime's parameters fulfill this condition and if $r = \pm a$ is in the stationary area, any particle can remain at rest there regardless of its charge. Comparing with (7), we obtain a rather reasonable requirement

$$q^2 < 4a^2. \tag{35}$$

Whether $r = \pm a$ is in the stationary area of the spacetime, as required by our ansatz, is given by the sign of $\Delta_r(r = \pm a)$ with (34) plugged in.

The negative solution is always in the stationary area, while the positive one further requires

$$m < \frac{4a^2 + 3q^2}{4a}. \tag{36}$$

The particles at $r = \pm a$ cannot be held in place by either electromagnetism (as the particles stay in place regardless of their charge) or a repulsive cosmological constant (as the required negative Λ is actually attractive) in an equilibrium with gravity. However, it can be shown that the two particles are never shielded by a horizon from the singularity, which thus acts as a naked singularity for them. This is in accord with the fact that naked singularities produce pockets of effectively repulsive gravity pushing the test particles away [25,26].

For static positions in the equatorial plane, we find instead

$$\frac{\Delta_r(r)}{r^4\tilde{s}\left(\Delta_r(r)-a^2\right)}\Big[\Lambda\tilde{s}r^5 - q\kappa\Lambda r^4 - \left(3m\tilde{s} + q\kappa(a^2\Lambda - 3)\right)r^2 + 3q(q\tilde{s} - 2\kappa m)r + 3q^3\kappa\Big] = 0 \tag{37}$$

with

$$\tilde{s} = \sqrt{\frac{\Delta_r(r) - a^2}{\rho^2(r, \theta = \pi/2)}}. \tag{38}$$

Again, instead of solving the above equation for r numerically, we can find the charge required to keep the particle static (this can only occur outside of the ergosphere)

$$\kappa = -\frac{\Lambda r^4 - 3mr + 3q^2}{3qr\tilde{s}}. \tag{39}$$

Although these particles do not have a vanishing angular momentum in general, this can happen with an additional condition on the spacetime parameters, namely $2\Lambda r^3 + \Lambda a^2 r + 3m = 0$.

5.2 Motion in the equatorial plane

We first focus on stationary circular orbits of both massive particles and photons before introducing an effective potential guiding the test particles around the black hole. With a constant angular velocity and no motion in the radial and axial directions, we are left with a single non-trivial equation of motion and the normalization of the four-velocity. Introducing

$$\Omega \equiv \frac{\mathrm{d}\phi}{\mathrm{d}t} = \frac{\dot{\phi}}{\dot{t}}, \tag{40}$$

these then reduce to an expression for $\dot{t}$

$$\dot{t} = \frac{3\Xi q\kappa r(a\Omega - 1)}{(\Lambda r^4 - 3mr + 3q^2)(a\Omega - 1)^2 + 3r^4\Omega^2} \tag{41}$$

and a single algebraic equation of degree 4 for Ω

$$\begin{aligned}&\Omega^4\Big[9a^2q^2\left(a^4+2a^2r^2+r^4-a^2\Delta_r\right)\kappa^2+3(2\Lambda a^2+3)r^8-18ma^2r^5\\&+18a^2q^2r^4+a^4P\Big]-\Omega^3\Big[18aq^2\left(2a^4+3a^2r^2+r^4-2a^2\Delta_r\right)\kappa^2\\&+4a\left(3\Lambda r^8-9mr^5+9q^2r^4+a^2P\right)\Big]+\Omega^2\Big[6\left(\Lambda r^8-3mr^5+3q^2r^4+a^2P\right)\\&+9q^2\left(6a^4+6a^2r^2+r^4-6a^2\Delta_r\right)\kappa^2\Big]-\Omega\Big[18aq^2\left(2a^2+r^2-2\Delta_r\right)\kappa^2\\&+4aP\Big]+\Big[9q^2\left(a^2-\Delta_r\right)\kappa^2+P\Big]=0\end{aligned}\tag{42}$$

with

$$P=\Lambda^2r^8-6\Lambda mr^5+6\Lambda q^2r^4+9m^2r^2-18mq^2r+9q^4.\tag{43}$$

While $\dot{\phi}$ and $\dot{t}$ are affected by the sign of the particle's charge κ, Ω is independent of it since there are no odd powers of κ in the above equation. Moreover, although we can have up to four different real values of Ω, the corresponding $\dot{t}$ may not necessarily be positive, which further reduces the number of physical solutions. There are regions admitting different numbers of physical solutions, both due to the number of real roots of (42) and the number of corresponding positive $\dot{t}$'s. It is of interest that there can also be an odd number of solutions as illustrated in Fig. 3.

For photon orbits we find a simple polynomial equation for the corresponding radius of the orbit

$$\begin{aligned}&3\Xi^2r^4+6m\left(\Lambda a^2-3\right)r^3+\left(27m^2-4\Lambda a^2q^2+12q^2\right)r^2\\&-12m\left(a^2+3q^2\right)r+12q^2\left(a^2+q^2\right)=0.\end{aligned}\tag{44}$$

It turns out that regardless of the values of the parameters in the metric, the real roots of the polynomial are always non-negative, barring circular photon orbits in the inner region of the spacetime with $r<0$. Moreover, there can always be either two or none such circular orbits and, if they exist, each orbit separates two adjacent regions admitting a different number of massive circular orbits, see Fig. 3.

In order to analyze general radial motion, we now establish an effective potential taking advantage of the integrals of motion (28) and the normalization equation. We easily find

$$\begin{aligned}\dot{t}=\frac{\Xi}{r^2\Delta_r}\Big[&-\Xi\left(a^2\Delta_r-(a^2+r^2)^2\right)E+a\Xi\left(\Delta_r-(a^2+r^2)\right)L\\&-(a^2+r^2)q\kappa r\Big],\end{aligned}\tag{45}$$

$$\dot{\phi}=\frac{\Xi}{r^2\Delta_r}\Big[-a\Xi\left(\Delta_r-(a^2+r^2)\right)E+\Xi\left(\Delta_r-a^2\right)L-aq\kappa r\Big].\tag{46}$$

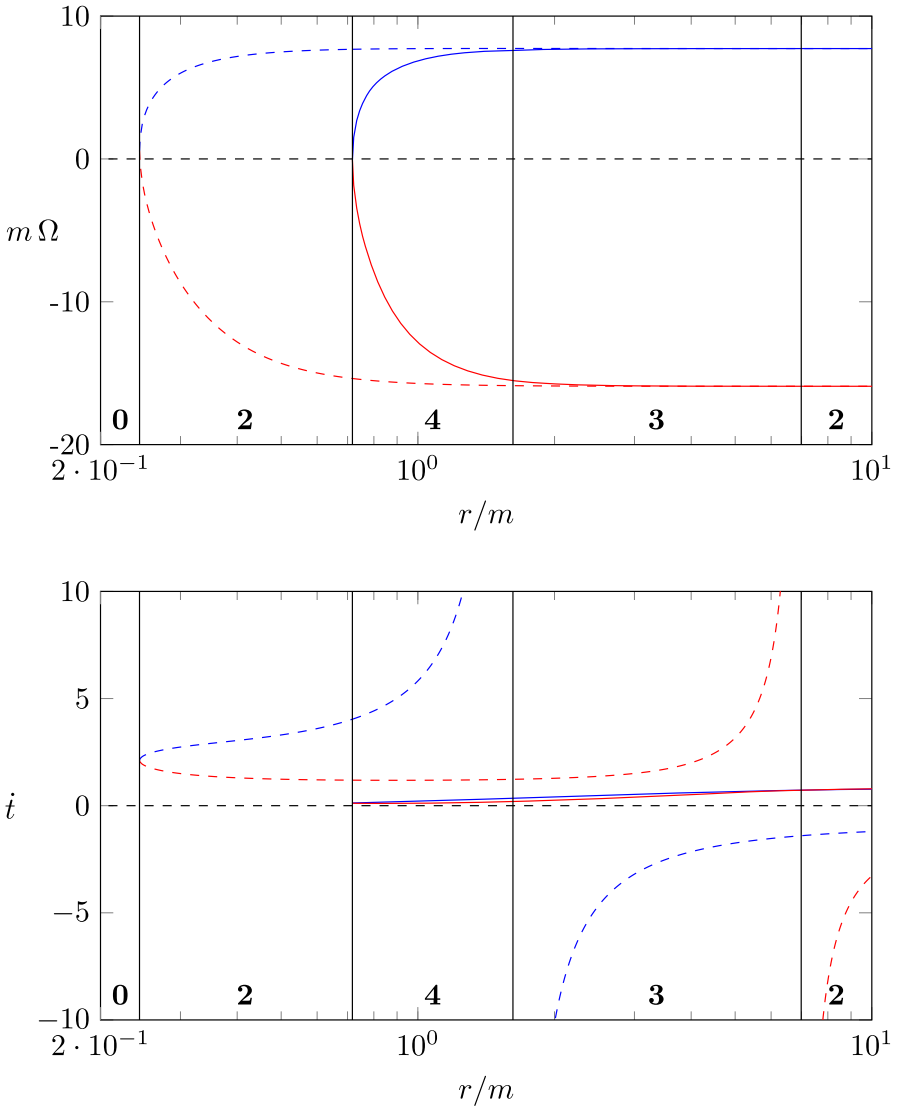

Fig. 3 Angular velocity Ω obtained from (42) and the corresponding $\dot{t}$ (in matching lines) as functions of the radius for the spacetime $\{\Lambda m^2, a/m, q/m\} = \{-324, 1/30, 2/9\}$ and a particle with $\kappa = 25$. Vertical lines separate regions with different numbers of physical solutions indicated by bold numbers and given by the requirement $\dot{t} > 0$ for a given Ω. Divergence of $\dot{t}(r)$ signifies a photon orbit, which solves (44)

From here, we express $\dot{r}$ as

$$\frac{1}{2}(\dot{r})^2 = -V(r; E, L, \kappa), \tag{47}$$

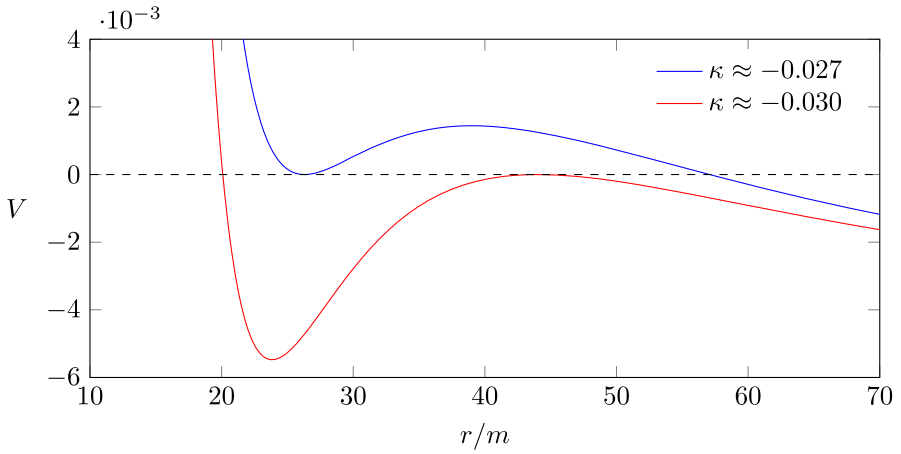

Fig. 4 A comparison of two effective potentials in a spacetime with parameters $\{\Lambda m^2, a/m, q/m\} = \{10^{-8}, 75, 5\}$ for two particles with the same $E = 1$ and $L = 15$ but different κ. The upper particle with a greater κ can be in a stable orbit at $r/m \approx 26$, the lower one in an unstable one at $r/m \approx 44$

where V is the sought effective potential,

$$V(r; E, L, \kappa) = \frac{q\kappa}{2r^3}\left(2\Xi\left(a^2 + r^2\right)E - 2\Xi aL - q\kappa r\right) - \delta\frac{\Delta_r(r)}{2r^2} + \frac{\Xi^2}{2r^4}\left(\left(\Delta_r(r) - (a^2 + r^2)\right)(aE - L)^2 - \left(a^2 + r^2\right)r^2E^2 + r^2L^2\right), \quad (48)$$

here δ is the four-velocity norm. The latter case has already been thoroughly analyzed in previous literature [27,28].

The turning points for a given particle are the roots of a sixth-degree polynomial, barring analytical solutions in the general case. Expanding the potential near an unstable ($\mathrm{d}^2V/\mathrm{d}r^2 < 0$) circular ($\mathrm{d}V/\mathrm{d}r = 0$) orbit, we find that approaching particles will get arbitrarily close to it in a finite time and they will wind ever closer exponentially. Inspecting the potential, we find that stable photon orbits (if there are any in the given spacetime) require

$$r < \frac{4}{3}\frac{q^2}{m}, \quad (49)$$

while unstable orbits satisfy the opposite inequality, confirming the well-known fact that photon orbits in the Schwarzschild and Kerr spacetimes are unstable [29]. As a side note, κ seems to have a considerable effect on the stability of orbits, see Fig. 4, where we consider two particles with the same integrals of motion but with different charge-to-mass ratios in the same spacetime. The divergence of the effective potential at $r = 0$ expelling any test particle from its vicinity is yet another manifestation of the already-discussed repulsive gravity for naked singularities.

To separate the potential, one can follow in the footsteps of [30]. V is quadratic in E and (48) can be recast as

$$V = -\frac{\Delta_r}{2r^2 N_{\rm eq}^2}\big(E - W_-\big)\big(E - W_+\big), \tag{50}$$

where

$$W_\pm = \frac{\Xi N_{\rm eq}^2}{r^2\Delta_r}\Bigg[\Big(a\Xi\big((a^2+r^2) - \Delta_r\big)L + \kappa q r(a^2+r^2)\Big) \pm \sqrt{r^2\Delta_r\left((r\Xi L - \kappa q a)^2 - \frac{r^2\Delta_r}{\Xi^2 N_{\rm eq}^2}\delta\right)}\Bigg] \tag{51}$$

and we use the lapse function

$$N^2 = -\frac{1}{g^{tt}} = -g_{tt} + \frac{(g_{t\phi})^2}{g_{\phi\phi}}, \tag{52}$$

which in the equatorial plane becomes

$$N_{\rm eq}^2 = \frac{r^2\Delta_r}{\Xi^2}\,\frac{1}{\big(a^2+r^2\big)^2 - a^2\Delta_r}\,. \tag{53}$$

The denominator of the last fraction coincides with the equatorial form of (22), which defines regions where closed timelike curves are present, and, therefore, the square of the lapse function is always positive unless we are either in a non-stationary region (where $\Delta_r < 0$) or within a CTC region. For instance, there is a stationary region around the singularity that contains CTC's and the lapse function is thus negative there. However, as proved in Sect. 4, the CTC region is always located below the inner black-hole horizon and, thus, if we exclude observers able to see the singularity and remain within the stationary region, the lapse function is well defined. Then, we have two contenders for the title of the separated potential, $W_- \leq W_+$, but only one of them represents physical particles moving forwards in time. Using (45) and the definitions above, we can further write

$$\dot{t} = \frac{(E - W_+) + (E - W_-)}{2N_{\rm eq}^2}, \tag{54}$$

and hence with $N_{\rm eq}^2 > 0$ relation $E \geq W_+$ automatically implies $E > W_-$ and we thus have both $V \leq 0$ and $\mathrm{sgn}(\dot{t}) > 0$, as required for physical particles. In case $E \leq W_- < W_+$, which would still yield the correct, negative sign of the potential, we get unphysical $\mathrm{sgn}(\dot{t}) < 0$, so we need to compare E to W_+. To conclude, W_+ is the correct separated potential.

Take note that in the part of the stationary area devoid of CTC's, the square root in $W_\pm$ is manifestly positive for massive particles ($\delta = -1$) and non-negative for photons ($\delta = 0$). Moreover, if $W_+ = W_-$, it is impossible to satisfy $E = W_+$, as then $\dot{t} = 0$. That means that there are no turning points for equatorial photons with $L = 0$. For $\Delta_r < 0$, we have $N_{\text{eq}}^2 < 0$ and the square root in $W_\pm$ is purely imaginary for massive and massless particles alike, which means there are no turning points in non-stationary regions.

To see that circular orbits and their stability can be determined using derivatives of W_+ instead of V, we first compute the first derivative of (50) and insert $E = W_+$ to obtain

$$\left.\frac{\mathrm{d}V}{\mathrm{d}r}\right|_{E=W_+} = \frac{\Delta_r}{2r^2 N_{\text{eq}}^2}\left(W_+ - W_-\right)\frac{\mathrm{d}W_+}{\mathrm{d}r}. \tag{55}$$

Apart from the horizons, the first derivative of W_+ therefore vanishes if and only if the particle follows a circular orbit. (Recall that considering $E = W_+$ prohibits $W_+ = W_-$.) Similarly, the second derivative yields

$$\left.\frac{\mathrm{d}^2V}{\mathrm{d}r^2}\right|_{\substack{E=W_+\\ W_+'=0}} = \frac{\Delta_r}{2r^2 N_{\text{eq}}^2}\left(W_+ - W_-\right)\frac{\mathrm{d}^2W_+}{\mathrm{d}r^2}, \tag{56}$$

which means that for circular orbits not only does the second derivative of W_+ vanish if V'' vanishes as well, but also that $\operatorname{sgn}(W_+'') = \operatorname{sgn}(V'')$. Expectedly, orbits located at minima of W_+ are, therefore, stable and those at maxima are unstable. For a discussion of stability of unrelated latitudinal motion, see, e.g., [31,32].

While the separated potential is more convenient for finding turning points, as it does not have to be redrawn every time one considers a particle with different E, its lengthy square root makes it less useful whenever derivatives are involved.

5.3 Radial motion along the axis of rotation

Due to the spacetime's symmetries, electrogeodesic equations permit a purely radial motion along the axis of rotation. The ϕ coordinate is degenerate on the axis and its value is inconsequential, and the equation for $\ddot{\theta}$ is trivial on the axis for initial $\dot{\theta} = 0$. We are left with two remaining equations of motion for t and r. Instead of solving the system, we again examine the corresponding effective potential (the simpler case of vanishing cosmological constant has been discussed in [33]). The situation here is simpler than in the equatorial plane as L vanishes for particles bound to the axis and, additionally, we can express $\dot{t}$ directly from E

$$\dot{t} = \frac{\Xi}{\Delta_r}\Big(\Xi\,\rho_0^2(r)E - rq\kappa\Big), \tag{57}$$

where

$$\rho_0^2(r) \equiv \rho^2(r, \theta \in \{0, \pi\}) = r^2 + a^2\,. \tag{58}$$

Substituting into the normalization equation, we obtain, similarly as before,

$$\frac{1}{2}(\dot{r})^2 = -V(r; E, \kappa) \tag{59}$$

with

$$V(r; E, \kappa) = -\frac{1}{2\rho_0^4(r)}\Big(\Xi\,\rho_0^2(r)E - q\kappa r\Big)^2 - \frac{\Delta_r(r)}{2\rho_0^2(r)}\,\delta. \tag{60}$$

This time, unlike in the equatorial plane, there is no infinite potential barrier at $r = 0$ unless $a = 0$. The physical situation is different, as for rotating black holes of the Kerr family there is no singularity on the axis in the used coordinates. Again, the potential can be separated as

$$V = -\frac{\Xi^2}{2}(E - W_-)(E - W_+) \tag{61}$$

with $W_- \leq W_+$ satisfying

$$W_\pm(r; \kappa) = \frac{1}{\Xi\,\rho_0^2}\left(q\kappa r \pm \sqrt{-\delta\Delta_r\rho_0^2}\right). \tag{62}$$

Following the same argument as in the equatorial plane, we again find that physical particles travelling forward in time are governed by W_+ and must satisfy $E \geq W_+$, and that potentials V and W_+ are equivalent not only when examining turning points, but also static positions and their stability. Analogously to the equatorial plane, the non-stationary regions with $\Delta_r < 0$ contain no turning points of timelike particles since $W_\pm$ are not real. Indeed, for $\Delta_r < 0$ and $\delta = -1$, (60) has no real roots.

Let us now analyze the stability of massive particles sitting at $r = \pm a$. Even though κ was irrelevant in the question of staticity, it turns out that it plays a crucial role for the stability of these particles: we obtain

$$\begin{aligned}\frac{\mathrm{d}^2V}{\mathrm{d}r^2}\bigg|_{r=\pm a} &= \frac{4a^2 - q^2}{8a^3}\sqrt{4a^2 \mp 4am + 3q^2}\,\frac{\mathrm{d}^2W_+}{\mathrm{d}r^2}\bigg|_{r=\pm a}\\ &= \frac{1}{4a^4}\left(\pm 2am + 2q^2 \mp q\kappa\sqrt{4a^2 \mp 4am + 3q^2}\right).\end{aligned} \tag{63}$$

Recall that $\Xi > 0$ implies $4a^2 > q^2$, see (35). Therefore, the threshold κ for which the particle stability changes is

$$\kappa^{\pm}_{\mathrm{thr}} = \frac{2\left(am \pm q^2\right)}{q\sqrt{4a^2 \mp 4am + 3q^2}}. \tag{64}$$

For $r = +a$ stable positions (in the minima of the potentials) require $q\kappa < q\kappa^{+}_{\mathrm{thr}}$ and unstable $q\kappa > q\kappa^{+}_{\mathrm{thr}}$. Curiously, for $r = -a$ the inequalities are swapped and stable positions require $q\kappa > q\kappa^{-}_{\mathrm{thr}}$, unstable $q\kappa < q\kappa^{-}_{\mathrm{thr}}$. The situation for $r = a$ is illustrated in terms of V in Fig. 5.

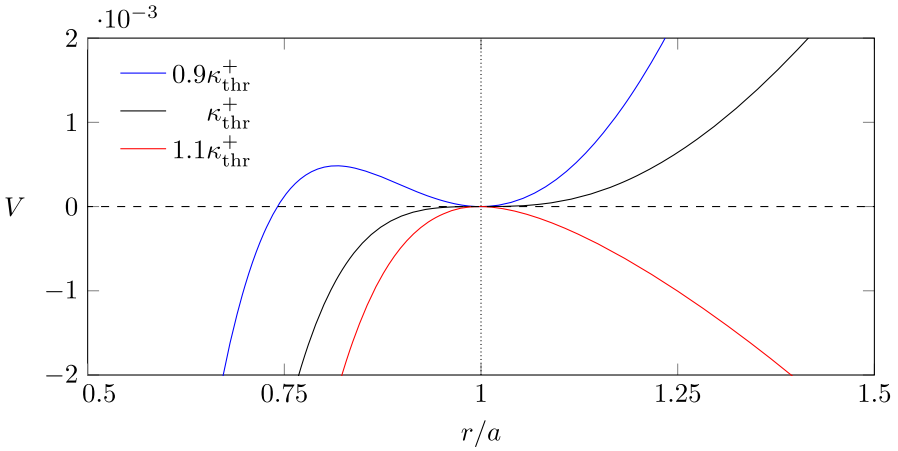

Fig. 5 The effective potentials V in a spacetime with parameters $\{\Lambda a^2, m/a, q/a\} = \{-12/49, 20/21, 4/7\}$ allowing for static particles at $r = \pm a$ for three particles differing by their charge and E. $\kappa^+_{\rm thr} = 47/\sqrt{129} \approx 4.14$, given by (64), is the charge-to-mass ratio of the middle particle with $E \approx 1.88$ and it represents a marginally stable static position. The upper particle with lower $q\kappa$ and $E \approx 1.75$ is in a stable static position and the lower particle with higher $q\kappa$ and $E \approx 2.01$ is in an unstable static position

Take note that for photons bound to the axis there are no turning points since the effective potential V is constant, $V = -\Xi^2 E^2/2 < 0$. Also note that it is impossible for these photons to have $E = 0$, as a quick inspection of (57) reveals that these photons would be frozen in time. From (57) it also follows that in stationary areas, $\mathrm{sgn}(\dot{t}) > 0$ actually requires $E > 0$. In the limit of $a = 0$ the potential leads to $\dot{r} = \pm E$, as is known for the Schwarzschild–anti-de Sitter spacetime [34]. For the radial coordinate velocity of a massless particle we obtain a remarkably simple formula

$$\frac{\mathrm{d}r}{\mathrm{d}t} = \pm \frac{\Delta_r(r)}{\Xi \rho_0^2(r)}, \tag{65}$$

which holds even for hypothetical charged massless particles because the particle's charge does not enter the normalization equation. In the general case $\mathrm{d}r/\mathrm{d}t$ cannot be integrated to obtain $r = r(t)$ in terms of elementary functions. However, should we take interest in null geodesics in the neighbourhood of a given horizon, we can Taylor-expand all the functions appearing in (65) in terms of $r - R_m$, where R_m is the position of the horizon of multiplicity m. The resulting formula can be integrated to yield an explicit dependance of radius, r, on coordinate time, t. For instance, for the triple horizon located at $r = R_3$ we find

$$r \approx \pm \frac{1}{\sqrt{\mp 2\zeta_3(R_3)\,(t - t_0)}} + R_3, \tag{66}$$

with

$$\zeta_3(R_3) = \frac{2}{3} \frac{\Lambda^2 R_3}{\left(\Lambda R_3^2 - 1\right)\left(5\Lambda R_3^2 - 3\right)} < 0. \tag{67}$$

The outer sign reflects whether the photon is above the horizon or below it while the inner sign distinguishes between photons approaching the horizon and receding from it.

5.4 The turnaround radius

Let us now mention the notion of the so-called turnaround, or static, radius as discussed in, e.g., [35,36]. This surface is well defined for spherically symmetric spacetimes, where radial geodesics only cross it either inwards or outwards but can never go back, and it has only been generalized for small deviations in [37]. The problem in the present case is that, generally, radial trajectories are not geodesics. The only exception are paths along the axis where a geodesic can be written in the required form $\ddot{r} - f(r) = 0$. Indeed, differentiating (59) with respect to the proper time, dividing by $\dot{r}$, and setting $\kappa = 0$ yields

$$\ddot{r} + \frac{1}{2}\frac{\mathrm{d}}{\mathrm{d}r}\left[\frac{\Delta_r}{r^2 + a^2}\right] = 0. \tag{68}$$

Since the numerator of $f(r)$ is a polynomial of degree 5 independent of the test particle's energy E, there are up to 5 different turnaround radii for particles moving along the axis. It is of interest that although the turnaround radii work locally, pushing away nearby originating geodesics, it is still possible for a geodesic to cross it in one direction, travel to a distant turnaround point given by $E = W_+$ with W_+ of (62), and then cross the local turnaround radius in the opposite direction than before. This suggests that the notion of turnaround radius is a local concept.

The closest analog of general radial geodesics are arguably geodesics of zero angular momentum. Let us explore the situation in the equatorial plane. Proceeding from (47) in analogy with the axial case, we again have an equation of the form $\ddot{r} - f(r, E) = 0$. This time, however, f depends on the energy so that the turnaround radius is not common to all test particles. The situation could still be saved if the dependance on E vanished for some r where the remaining term independent of E would vanish as well so that $f(r, E)$ would factor out. This however, is not the case apart from a special combination of the 4 spacetime parameters (a 3-dimensional subspace). Put differently, there is no particular turnaround radius shared by all members of the KN(a)dS spacetime family.

6 Conclusions

In this paper we reviewed the properties of the most general electrovacuum axially symmetric black-hole spacetime, the Kerr–Newman–(anti-)de Sitter solution of the Einstein–Maxwell equations. This is an exact solution that can include even a horizon of degree three arising due to the merging of three originally separate single horizons. The structure of the spacetime is more varied than in the case of its simpler cousins and, in this paper, we presented the extreme cases. One can naturally ask what happens if a particle is dropped inside the black hole, perturbing the parameters of the spacetime. We discussed how the horizons split or merge during such a process. We studied closed

timelike curves and the regions where they can occur. Our main focus, however, was on electrogeodesics. We proceeded from the integrals of motion and investigated the most interesting trajectories, namely the positions of static test particles and general paths in the equatorial plane and along the axis. To facilitate the discussion, we introduced an effective potential, which enables us to distinguish the allowed and forbidden regions for motion of specific charged test particles. Lastly, we briefly discussed the turnaround radii in this spacetime.

Thus far, our work has only involved test particle motion, that is, the paths of charged particles moving in the gravitational and electromagnetic fields generated purely by the black hole. It is, however, clear that the particle generates its own fields as well. On a curved background, even the electrostatic field of a point particle influences its motion through a non-vanishing self force. In our future work, we thus plan to include the back reaction of the Maxwell field generated by the test particle on its very motion as well.

Acknowledgements J.V. was supported by Charles University, Project GA UK 80918. M.Ž. acknowledges support by GACR 17-13525S.

References

1. Carter, B.: Black hole equilibrium states. In: DeWitt, B.S., DeWitt, C. (eds.) Black Holes (1972 Les Houches Lectures). Gordon and Breach, New York (1973)
2. Hagihara, Y.: Theory of the relativistic trajectories in a gravitational field of Schwarzschild. Jpn. J. Astron. Geophys. **8**, 67 (1930)
3. Carter, B.: Global structure of the Kerr family of gravitational fields. Phys. Rev. **174**, 1559–1571 (1968). https://doi.org/10.1103/PhysRev.174.1559
4. Chandrasekhar, S.: The Mathematical Theory of Black Holes. Oxford University Press, New York (1983)
5. Cebeci, H., Özdemir, N., Şentorun, S.: Motion of the charged test particles in Kerr–Newman–Taub-NUT spacetime and analytical solutions. Phys. Rev. D **93**, 104031 (2016). https://doi.org/10.1103/PhysRevD.93.104031
6. Soroushfar, S., Saffari, R., Kazempour, S., Grunau, S., Kunz, J.: Detailed study of geodesics in the Kerr–Newman–(A)dS spacetime and the rotating charged black hole spacetime in $f(R)$ gravity. Phys. Rev. D **94**, 024052 (2016). https://doi.org/10.1103/PhysRevD.94.024052
7. Hackmann, E., Xu, H.: Charged particle motion in Kerr–Newmann space-times. Phys. Rev. D **87**(12), 124030 (2013). https://doi.org/10.1103/PhysRevD.87.124030
8. Gibbons, G.W., Hawking, S.W.: Cosmological event horizons, thermodynamics, and particle creation. Phys. Rev. D **15**, 2738–2751 (1977). https://doi.org/10.1103/PhysRevD.15.2738
9. Griffiths, J.B., Podolský, J.: Exact Space-Times in Einstein's General Relativity. Cambridge University Press, Cambridge (2009)
10. Aghanim, N., et al.: Planck 2018 results. VI. Cosmological parameters. https://arxiv.org/pdf/1807.06209.pdf (2018). Accessed 17 June 2019
11. Lauer, T.R., et al.: The masses of nuclear black holes in luminous elliptical galaxies and implications for the space density of the most massive black holes. Astrophys. J. **662**, 808–834 (2007). https://doi.org/10.1086/518223
12. Veselý, J.: Charged particles in space-times with an electromagnetic field. Master's thesis, Charles University, Prague. https://dspace.cuni.cz/bitstream/handle/20.500.11956/90577/DPTX_2015_1_11320_0_484776_0_170034.pdf (2017). Accessed 22 October 2018
13. Cardoso, V., Gualtieri, L.: Testing the black hole 'no-hair' hypothesis. Class. Quant. Grav. **33**(17), 174001 (2016). https://doi.org/10.1088/0264-9381/33/17/174001
14. Nielsen, A.B.: On the distribution of stellar-sized black hole spins. J. Phys. Conf. Ser. **716**(1), 012002 (2016). https://doi.org/10.1088/1742-6596/716/1/012002

15. Middleton, M.: Black hole spin: theory and observation, Chapter 3. In: Bambi, C. (ed.) Astrophysics of Black Holes: From Fundamental Aspects to Latest Developments, pp. 99–151. Springer, Berlin (2016)
16. Gou, L., McClintock, J.E., Reid, M.J., Orosz, J.A., Steiner, J.F., Narayan, R., Xiang, J., Remillard, R.A., Arnaud, K.A., Davis, S.W.: The extreme spin of the black hole in Cygnus X-1. Astrophys. J. **742**, 85 (2011). https://doi.org/10.1088/0004-637X/742/2/85
17. Stuchlík, Z., Slaný, P.: Equatorial circular orbits in the Kerr–de Sitter spacetimes. Phys. Rev. D **69**, 064001 (2004). https://doi.org/10.1103/PhysRevD.69.064001
18. Gibbons, G.W., Shellard, E.P.S., Rankin, S.J.: The Future of Theoretical Physics and Cosmology: Celebrating Stephen Hawking's Contributions to Physics. Cambridge University Press, Cambridge (2003)
19. Monroe, H.: Are causality violations undesirable? Found. Phys. **38**, 1065–1069 (2008). https://doi.org/10.1007/s10701-008-9254-9
20. Andreka, H., Nemeti, I., Wuthrich, C.: A Twist in the geometry of rotating black holes: seeking the cause of acausality. Gen. Relativ. Gravit. **40**, 1809–1823 (2008). https://doi.org/10.1007/s10714-007-0577-1
21. de Felice, F., Calvani, M.: Causality violation in the Kerr metric. Gen. Relativ. Gravit. **10**, 335–342 (1979). https://doi.org/10.1007/BF00759491
22. de Felice, F., Nobili, L., Calvani, M.: Charged singularities: the causality violation. J. Phys. A **13**, 3635–3641 (1980). https://doi.org/10.1088/0305-4470/13/12/012
23. Goldstein, H., Poole, C., Safko, J.: Classical Mechanics, 3rd edn. Addison-Wesley, Boston (2000)
24. Hackmann, E., Lämmerzahl, C., Kagramanova, V., Kunz, J.: Analytical solution of the geodesic equation in Kerr–(anti) de Sitter space-times. Phys. Rev. D **81**, 044020 (2010). https://doi.org/10.1103/PhysRevD.81.044020
25. Luongo, O., Quevedo, H.: Characterizing repulsive gravity with curvature eigenvalues. Phys. Rev. D **90**(8), 084032 (2014). https://doi.org/10.1103/PhysRevD.90.084032
26. Boshkayev, K., Gasperin, E., Gutiérrez-Piñeres, A.C., Quevedo, H., Toktarbay, S.: Motion of test particles in the field of a naked singularity. Phys. Rev. D **93**(2), 024024 (2016). https://doi.org/10.1103/PhysRevD.93.024024
27. Stuchlík, Z., Hledík, S.: Equatorial photon motion in the Kerr–Newman spacetimes with a non-zero cosmological constant. Class. Quant. Grav. **17**, 4541–4576 (2000). https://doi.org/10.1088/0264-9381/17/21/312
28. Stuchlík, Z., Bao, G., Ostgaard, E., Hledík, S.: Kerr–Newman–de Sitter black holes with a restricted repulsive barrier of equatorial photon motion. Phys. Rev. D **58**, 084003 (1998). https://doi.org/10.1103/PhysRevD.58.084003
29. Cunha, P.V.P., Herdeiro, C.A.R., Radu, E.: Fundamental photon orbits: black hole shadows and spacetime instabilities. Phys. Rev. D **96**(2), 024039 (2017). https://doi.org/10.1103/PhysRevD.96.024039
30. Hejda, F., Bičák, J.: Kinematic restrictions on particle collisions near extremal black holes: a unified picture. Phys. Rev. D **95**(8), 084055 (2017). https://doi.org/10.1103/PhysRevD.95.084055
31. De Felice, F., Calvani, M.: Orbital and vortical motion in the Kerr metric. Nuovo Cim. B **10**, 447–458 (1972)
32. Stuchlík, Z.: The motion of test particles in black-hole backgrounds with non-zero cosmological constant. Bull. Astron. Inst. Czech. **34**, 129–149 (1983)
33. Bičák, J., Stuchlík, Z., Balek, V.: The motion of charged particles in the field of rotating charged black holes and naked singularities. Bull. Astron. Inst. Czech. **40**, 65–92 (1989)
34. Cruz, N., Olivares, M., Villanueva, J.R.: The geodesic structure of the schwarzschild anti-de Sitter black hole. Class. Quant. Grav. **22**, 1167–1190 (2005). https://doi.org/10.1088/0264-9381/22/6/016
35. Stuchlík, Z., Hledík, S.: Some properties of the Schwarzschild-de Sitter and Schwarzschild-anti-de Sitter spacetimes. Phys. Rev. D **60**, 044006 (1999). https://doi.org/10.1103/PhysRevD.60.044006
36. Faraoni, V., Lapierre-Léonard, M., Prain, A.: Turnaround radius in an accelerated universe with quasi-local mass. J. Cosmol. Astropart. Phys. **2015**(10), 013–013 (2015). https://doi.org/10.1088/1475-7516/2015/10/013
37. Giusti, A., Faraoni, V.: Turnaround size of non-spherical structures. Phys. Dark Univ. **26**, 100353 (2019). https://doi.org/10.1016/j.dark.2019.100353